encit 2020

ABCM Associação Brasileira de Engenharia e Ciências Mecânicas

18th Brazilian Congress of Thermal Sciences and Engineering
November 16-20, 2020 (Online)

ENC-2020-0149

AN EXPERIMENTAL INVESTIGATION OF ACOUSTICAL SIMILARITY IN LARGE-SCALE INDUSTRIAL AXIAL FANS

Víctor Leonardo Moura Vieira da Silva
William Roberto Wolf
Universidade Estadual de Campinas, UNICAMP, 13083-860, Campinas, SP, Brasil
victorleonnardo@gmail.com
wolf@fem.unicamp.br

Abstract: *This work presents an experimental study of acoustical similarity performed for a large-scale axial fan designed to operate in air cooled condensers (ACC) of power plants. The main goal of this work is to obtain the relevant empirical parameters which are necessary in the acoustic similarity analysis. We also investigate their behavior when fan blade angle of attack and airflow conditions are changed. The empirical parameters studied are the exponent of Mach number term and a spectral function that depend on the airflow rate and fan geometry. In order to make this possible, the experiments are performed in a full-size test station where the airflow, static pressure, shaft power and sound pressure level (SPL) are measured. The fan sound power level (PWL) is then calculated using the fan SPL measurements and a reference sound source. In order to validate the acoustic similarity approach, the PWL frequency spectra calculated using the rotational speed is compared to results of the experiment at the same rotational speed. A discussion on the influence of the fan operation conditions in the empirical parameters is also presented.*

Keywords: *axial fan, acoustic similarity, industrial ventilation*

NOMENCLATURE

D_D	:	Acoustic energy density from direct sound field
D_R	:	Acoustic energy density from reverberant sound field
D_T	:	Total acoustic energy density in test station
$K_{t,Fan}$	:	Weather correction from fan test
$K_{t,RSS}$	:	Weather correction from RSS test
$L_{p,Fan}$	:	SPL of fan
$L_{p,RSS}$	:	SPL of the RSS
$L_{pi,RSS}$	:	SPL of RSS in microphone position i
$L_{w\,O,Calc}$	:	Overall PWL calculated
$L_{w\,O,Fan}$	:	Overall PWL of fan
$L_{w,Calc}$	:	Calculated PWL
$L_{w,Fan}$	:	PWL of fan
$L_{w,RSS}$	:	PWL of the reference sound source
Q_f	:	Air flow rate
U_T	:	Velocity of blade tip
q_T	:	Dynamic pressure at blade tip
D	:	Fan diameter
Q	:	Directive factor
R	:	Room's constant from Sabine's formula
SP	:	Fan static pressure
W	:	Acoustic power
c	:	Velocity of sound propagation
d	:	Distance between RSS and mic. position
f	:	Frequency
k	:	Octave bands
p	:	Root mean square of sound pressure
r	:	Observer distance from source
ΔL_f	:	Indicator of reverberant sound field from ISO3747
β	:	Mach number coefficient
ρ	:	Air density
φ	:	Air flow rate coefficient
ψ	:	Static pressure coefficient
Ω	:	Fan rotational speed

Dimensionless parameters

He	:	Helmholtz number
Ma	:	Mach number of blade tip
Re	:	Reynolds number
St	:	Strouhal number

Abbreviations

AMCA	:	Air Movement and Control Association
ANG 1	:	Pitch angle 1 at blade tip of the fan
ANG 2	:	Pitch angle 2 at blade tip of the fan
AoA	:	Angle of Attack
PWL	:	Sound Power Level ($W_{ref} = 10$pW)
RPM 1	:	Rotation speed 1 of the fan
RPM 2	:	Rotation speed 2 of the fan
SPL	:	Sound Pressure Level ($p_{ref} = 20$μPa)
cv	:	Range of airflow coefficient values

1. INTRODUCTION

Industrial ventilation finds several applications in engineering, including public transportation, mining and energy generation, and reducing fan noise is one of the main challenges for design of efficient fan configurations. In the present work, a study of acoustic similarity for large-scale industrial axial fans is shown considering differences in operation conditions, e.g., airflow and static pressure variations. The acoustic similarity of turbomachinery depends of a particular spectrum function calculated by experimental measurements. Such function is important since it allows a scaling of acoustic spectra with respect to different rotation speeds and fan diameters. The main goal of this work is to understand how this scaling changes by modifications of other similarity parameters such as pitch angle of fan blades and airflow coefficient for large-scale axial fans.

In order to obtain the scaling, we perform a set of acoustic experiments varying static pressure, airflow and power of a fan with 10,97 m of diameter in a full-scale test station. The acoustical data is presented in terms of sound power level (PWL) of the fan in octave bands from 125Hz to 8000 Hz as a function of flow parameters which are presented as dimensionless coefficients. The fan PWL is calculated from sound pressure level (SPL) measurements in accordance with the ISO3747 procedure. The measurements were possible thanks to Fan Technology Resources company that kindly made available its infrastructure and funded the full experimental campaign. Hence, all measured values are presented in non-dimensional units in order to protect intellectual property of the company. Anyway, this is a standard procedure and does not prevent the main objective of this work, which is the scaling study.

The remainder of this paper is organized as follows: we start with a discussion about acoustic the2ory and its connection with the ISO3747 procedure followed by considerations on the acoustic characterization of the test station. Further corrections by weather conditions are also shown since the test station is located outdoors. Then, the theory of acoustic similarity is applied supported by the experimental results, and frequency spectra of PWL is compared to experimental results for different rotational speeds scaled in order to validate the acoustic similarity assumptions.

2. THEORETICAL MODELS AND EXPERIMENTAL METHODS

The test station where experiments are performed is shown in Figure 1. The airflow is measured inside the test station by a 3D anemometer placed at 40 measurement points following AMCA 210-16 (2016) recommendations. The static pressure data is collected by relative pressure probes at 4 measurement points. The shaft power is calculated using the torque measured on the fan shaft and the fan rotational speed measured at the same time.

Figure 1: Full-scale fan test station of Fan Technology Resources.

The acoustic field generated by the fan operating inside the test station achieves steady-state conditions around 0.25s as further described by Kinsler et al (2000). According to Barron (2001), for steady-state conditions, the acoustic sound field at the test station may be divided into two components: 1) The *direct sound field*, which consists of acoustic energy associated with sound waves that come directly to observer without any reflection, and 2) The *reverberant sound field*, consisting of acoustic energy associated with sound waves that come to observer after reflections in various surfaces (walls, fan, etc) inside the test station. The total acoustic energy density at the room in steady-state condition is the sum of the contributions due the direct and reverberant sound fields as:

$$D_T = D_R + D_D = \frac{4W}{cR} + \frac{QW}{4\pi r^2 c} = \frac{W}{c}\left(\frac{4}{R} + \frac{Q}{4\pi r^2}\right) = \frac{p^2}{\rho c^2}, \tag{1}$$

where:

R : room's constant, obtained from Sabine's formula (Barron, 2001).

The ISO 3747 (2010) standard uses the comparison method to determine the sound power level, which can be used if the room provides a reverberant sound field. It means that the term referring to the reverberant field is much higher than the term referring to direct field, therefore:

$$\frac{4}{R} + \frac{Q}{4\pi r^2} \approx \frac{4}{R}$$

However, R is constant and only depends of the room characteristics (sound absorption, surface area, etc) thus, it is possible to use the comparison method for reverberant rooms as described by the ISO3747 and related by Eq. (2). The fan PWL is calculated taking both SPL measurements from fan and reference sound source (RSS) by applying Eq. (2). It considers a RSS that emits noise for each octave with a known PWL. The resulting SPL is then measured at several points along the test station radius and the RSS is replaced by the fan. The fan SPL is also measured for each octave band at the same measurement points of the RSS SPL evaluation. In Eq. (2), the terms K_t on the right hand side contain, respectively, the characteristic impedance of the air in the day of the RSS and fan measurements. If both tests are conducted in the same day, it is possible that weather changes can be neglected. However, since it is likely that the tests are performed in different days, weather corrections must be taken into account as suggested below.

$$L_{w,Fan} = L_{w,RSS} - L_{p,RSS} + L_{p,Fan} + K_{t,RSS} - K_{t,Fan}\ , \tag{2}$$

To make sure that the microphones are positioned in a reverberant sound field, the value of indicator (ΔL_f) shall be higher than 7 and the background noise of the test environment must be sufficiently low. Higher values of ΔL_f indicate a more reverberant sound field and lower measurement uncertainties. Therefore, this parameter defines if the environment is reverberant enough to avoid errors in the measurement due to the different directivity of the reference sound source and fan. The ISO3747 (2010) says that values of $\Delta L_f \geq 7$ provide an uncertainty of 1,5 dB in the measurements. The ΔL_f indicator is calculated for each octave band and measurement position using Eq. (3), where d is the distance between the reference sound source and the microphone position ($d_0 = 1$ m). All 20 measurement points are into a reverberant sound field.

$$\Delta L_f = L_{p,RSS} - L_{w,RSS} + 11\ \text{dB} + 20\log\left(\frac{d}{d_0}\right)[\text{dB}]\ . \tag{3}$$

In acoustic similarity analyses, to compare results among different fan operation points, dimensionless coefficients are often used instead of dimensional values of flow rate and static pressure. According to the fan law presented by Bleier (1997), the flow and static pressure coefficients can be obtained through Eqs. (4) and (5) as

$$\varphi = \frac{Q_f}{D^3\left(\frac{\Omega}{60}\right)}, \quad \text{and} \tag{4}$$

$$\psi = \frac{SP}{\rho D^2\left(\frac{\Omega}{60}\right)^2}\ . \tag{5}$$

There are another dimensionless parameters which should be introduced for a complete comprehension of the acoustic similarity analysis in this work, described in the equations below. They are respectively, the Mach Number at the blade tip, and the Strouhal and Helmholtz numbers. The Mach number provides a measure in terms of flow compressibility at the blade tip. While the Strouhal number provides a non-dimensional frequency as a function of the fan rotation, the Helmholtz number gives an estimate of the source compactness.

$$Ma = \frac{U_T}{c}, \tag{6}$$

$$St = \frac{2\pi f}{\Omega}, \tag{7}$$

$$He = \frac{fD}{c}. \tag{8}$$

The velocity U_T and dynamic pressure q_T at the blade tip can be calculated by Eqs. (9) and (10), respectively

$$U_T = \frac{\pi D\Omega}{60}, \tag{9}$$

$$q_T = \frac{\rho U_T^2}{2}. \tag{10}$$

Neise and Barsikow (1982) studied the sound radiation from three geometrically similar centrifugal fans with diameters of 140, 280 and 560 mm, and their results show that the influence of Reynolds number could be neglected for a range $1{,}4\text{x}10^5 < \text{Re} < 2{,}2\text{x}10^6$. Their work suggests that the acoustic system response for the fan is a function of the Helmholtz number (He), *D/r* ratio, flow coefficient (φ) and Strouhal (*St*) number. Here, *r* is the distance between source and observer and *D* is the fan diameter. However, more recently, Cattanei and Canepa (2011) found a dependence of Reynolds number in their experiments. These authors also studied the similarity of shrouded axial fans and obtained a spectral function that allows scaled SPLs to other rotation speeds and diameters. Blake (2017) suggests Eq. (11) as a fan law of acoustic similarity, which takes into account various mechanisms of aerodynamic sound generation since the flow coefficient and distance of observer are kept the same. The author says that β is a function of airflow coefficient and, for most cases, it would be a factor of 2. However, in this work, we find other values of β- but close to 2 - as function of airflow coefficient. Cattanei and Canepa (2011) also found different values of β in their work. Equation (11) for the fan law of acoustic similarity is given by

$$p^2(\boldsymbol{x}, f) = q_T^2 Ma^{\beta(\varphi)} \left(\frac{D}{r}\right)^2 F(St, \varphi) G(He)\,, \tag{11}$$

The term $G(He)$ is a function of the Helmholtz number and represents an acoustic system response function such as acoustic resonance and radiation properties of the fan. The function $F(St)$ provides the dimensionless frequency spectrum of the dipolar source strength based on the Strouhal number. This function describes the aeroacoustic sources on the fan as said by Neise and Barsikow (1982). The main advantage of having the PWL spectrum of the fan is the simplification of the test station as a source point and a receiver located in the acoustic far-field at a distance r, sufficiently far so that sound waves reach the observer as plane waves, so the radiated sound power can be calculated using Eq. (12). This allows considering that all resonance and radiation properties of the fan have already been accounted for in the PWL calculation, so $G(He) = 1$

$$W = \frac{p^2 4\pi r^2}{\rho c}\,. \tag{12}$$

Substituting Eq. (12) in Eq. (11), and using $W_{ref} = 1$ pW, the PWL can be calculated using Eq. (13) given by

$$L_{w,Calc}(f) = 20\log_{10} q_T D + 10\beta(\varphi)\log_{10} Ma + 10\log_{10} F(St, \varphi) + \log_{10}\frac{4\pi}{W_{ref}\rho c} \tag{13}$$

where, the frequencies are chosen as f =125 Hz, 250 Hz, 500 Hz, 1000 Hz, 2000 Hz, 4000 Hz and 8000 Hz.

Experimental data of $L_{w,Fan}(f)$ were measured with fan operating at RPM 1 and RPM 2 in order to obtain the values of $\beta(\varphi)$ and $F(St, \varphi)$. Using Eq. (13) for each octave band it is possible to make $L_{w,Calc}(f) = L_{w,Fan}(f)$, yielding the following equation

$$10\log_{10} F(St, \varphi) = L_{w,Fan,1}(f) - 20\log_{10} q_{T,1} D - 10\beta(\varphi)\log_{10} Ma_1 - \log_{10}\frac{4\pi}{W_{ref}\rho c}\,, \tag{14}$$

where it is possible to substitute Eq. (14) in Eq. (13), and, then, use RPM 2 conditions to yield

$$L_{w,Calc,2}(f) = 20\log_{10}\frac{q_{T,2} D_2}{q_{T,1} D_1} + 10\beta(\varphi)\log_{10}\frac{Ma_2}{Ma_1} + L_{w,Fan,1}(f)\,. \tag{15}$$

In the previous equations, the subscripts 1 and 2 refer to RPM 1 and RPM 2, respectively. It is possible to obtain $\beta(\varphi)$ just making $L_{w,Calc,2}(f) = L_{w,Fan,2}(f)$ band by band, but this would make $\beta(\varphi)$ a frequency dependent function, which is not true. However, the uncertainty of experiment due random errors is responsible to produce values of $\beta(\varphi)$ for each individual frequency. Hence, in order to keep the acoustic similarity of the fan and taking into account all random source errors, it is suitable to assume that the overall PWL calculated for RPM 2 might be the same of the overall PWL measured at RPM 2. Equation (16) can be used to calculate the overall PWL for all octave bands as

$$L_{w\,O,Fan} = 10\log_{10}\sum_{k=1}^{n} 10^{0{,}1\left(L_{w,Fan(k)}\right)}\,. \tag{16}$$

Considering $L_{w\,O,Calc,2} = L_{w\,O,Fan,2}$ and calculating the overall PWL for both sides of Eq. (15), $\beta(\varphi)$ can be calculated using Eq. (17), and $F(St, \varphi)$ is obtained substituting $\beta(\varphi)$ in Eq. (14).

$$\beta(\varphi) = \frac{10\log_{10}\sum_{k=1}^{n} 10^{0,1\left(L_{w,Fan,2}(k)\right)} - 20\log_{10}\frac{q_{T,2}D_2}{q_{T,1}D_1} - 10\log_{10}\sum_{k=1}^{n} 10^{0,1\left(L_{w,Fan,1}(k)\right)}}{10\log_{10}\frac{Ma_2}{Ma_1}}. \quad (17)$$

3. RESULTS

The procedure described above is used to obtain the $\beta(\varphi)$ and $F(St,\varphi)$ functions for each one of the airflow coefficients for two different angles of the blade. Blade angle 2 is four degrees higher than blade angle 1, and they are going to be described as ANG 2 and ANG 1, respectively, from now on. As said before, the experiments and acoustic similarity analyses are performed with fan operating in two rotational speeds, RPM 1 and RPM 2, where RPM 2 is 17% higher than RPM 1. The goal of this work is to understand the behavior of the $\beta(\varphi)$ and $F(St,\varphi)$ functions when the flow coefficient or blade angle is changed. Hence, the results are initially presented considering the aerodynamic performance of the fan and, then, the measured PWL followed by the behavior of $\beta(\varphi)$ and $F(St,\varphi)$.

Figure 2 shows the chart of static pressure coefficients as a function of the airflow coefficient for the two blade angles. These coefficients are calculated by the static pressure, airflow, rotational speed and density, measured at the experiments with fan operating at RPM 1 and then with RPM 2, at the same time of the acoustic measurements. Notice that the operational points are matching when the rotational speed is changed, because of the aerodynamic similarity represented by the static pressure and airflow coefficients. As described before the acoustic similarity analysis should be made considering acoustic measurements at the same air flow coefficient of RPM 1 and RPM 2 test. Hence, as was not possible to have the exactly the same air flow coefficient, it was established ranges of flow coefficient values allowing the comparison between the blade angles and the determination of $\beta(\varphi)$ and $F(St,\varphi)$. The five ranges of flow coefficient are related in Figure 2 from cv1 up to cv5 and, it was considered that $\beta(\varphi)$ and $F(St,\varphi)$ are not changing with air flow coefficient (φ) inside of each cv range delimited by the brackets. This assumption is necessary to make possible the acoustic similarity analysis because it is difficult to achieve the same point of airflow coefficient during the tests.

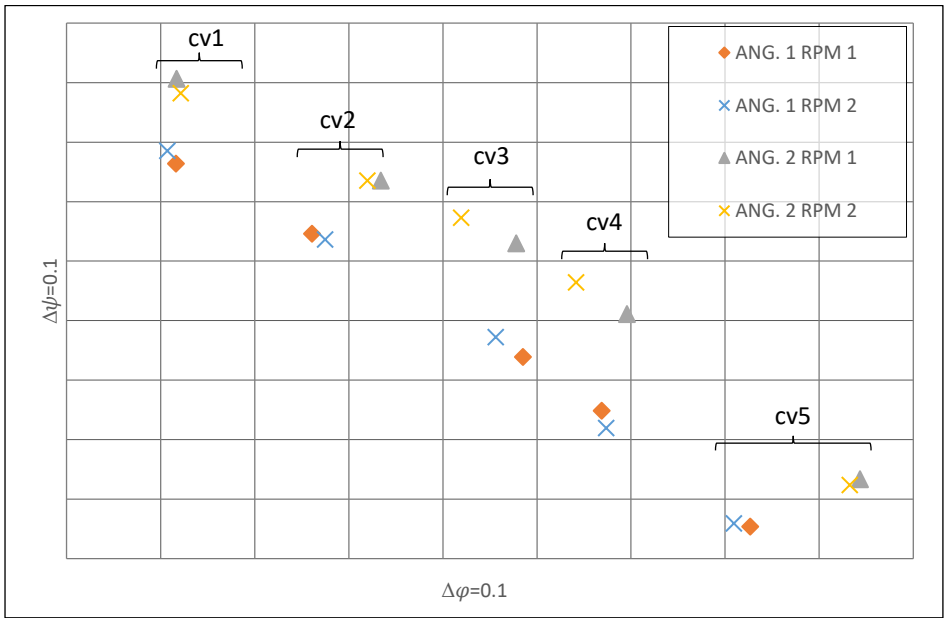

Figure 2: Experimental chart of static pressure and air flow, expressed through dimensionless coefficients.

The experimental data of PWL are presented in Figure 3 for both blade pitch angles and rotational speeds. At low frequencies, i.e., 125 Hz and 250 Hz, there are no significant variation of PWL values comparing the different cv points. From middle frequencies on, the PWL values increase for all cases when cv values decrease. The figure shows that noise levels are increased with the rotational speed, as expected. One can see that the high frequencies have a larger disparity comparing the two pitch angles of the blade while keeping the same rotation speed. In this case, the radiated acoustic energy increases with AoA. This is a typical behavior of fans since the importance of noise sources from turbulent boundary layers and their subsequent scattering at the trailing edge increase with AoA. The high frequency noise is dominated by such sources. This analysis show that the experimental PWL data are consistent, describing the expected acoustical behavior of fans and providing reliable data needed to calculate the PWL to study the behavior of the $\beta(\varphi)$ and $F(St,\varphi)$ functions.

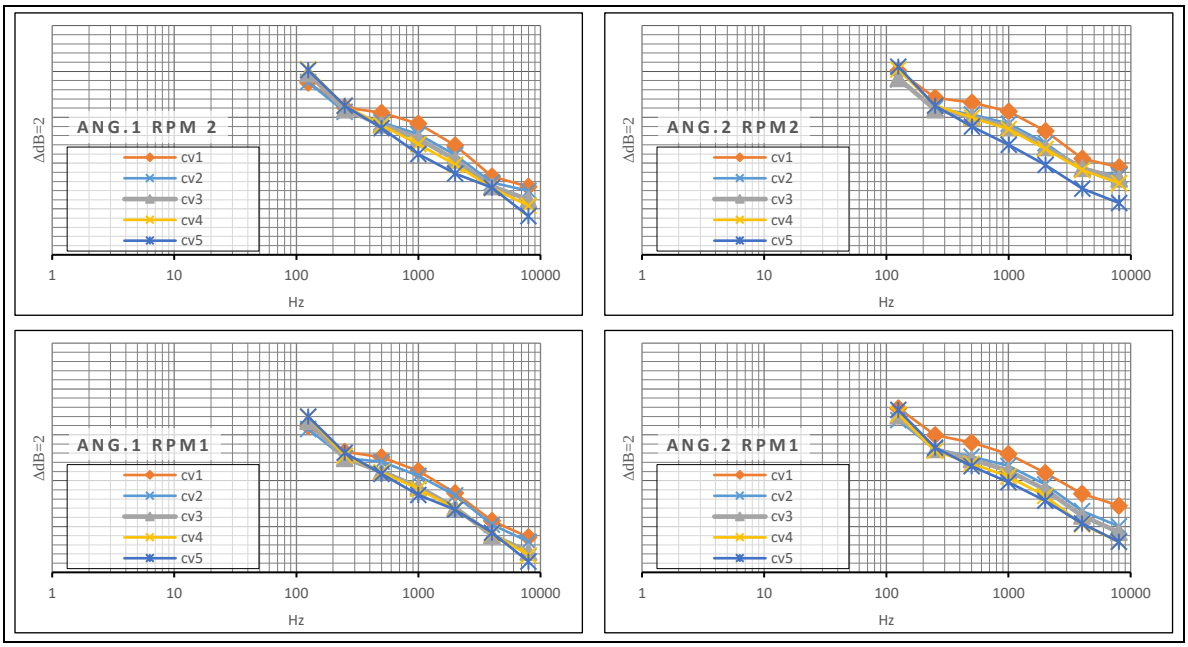

Figure 3: Experimental data of fan PWL for each experiment.

The values obtained for the Mach coefficient $\beta(\varphi)$ are shown in Figure 4. This variable is a function of airflow coeficient and blade angle and it has an important contribuition to the accuracy of the fan PWL scaling. It is almost a linear function of airflow coeficient but, as can seen, there is a small dispersion of the data arround the fiting line. It can be noticed that $\beta(\varphi)$ values for ANG 2 are lower compared to ANG 1, and their slopes are similar after a linear fit is applied. Values of β= 2 are suggested by Blake (2017) for acoustic similarity analysis of fans. Indeed, this value is relativaly close to those presented in Fig. 4, but keeping β = 2 for all air flow coefficients would lead to 1.8 dB error in the overrall PWL calculated, considering both pitch angles.

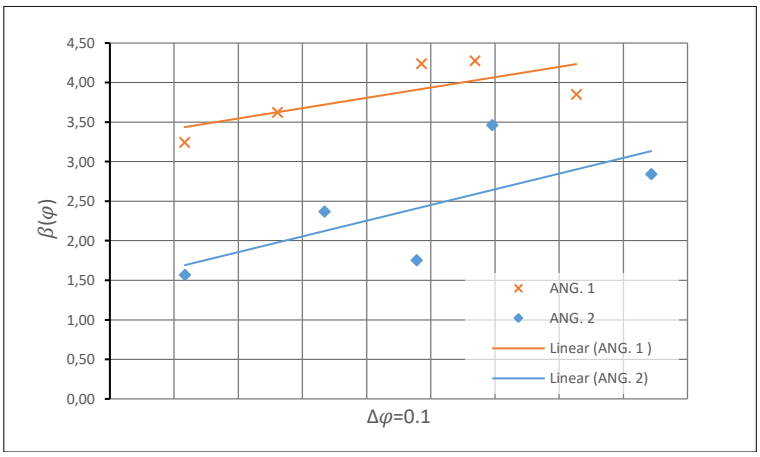

Figure 4: Mach number coefficient $\beta(\varphi)$ as a function of airflow coefficient.

Figure 5 shows the results of PWL spectra scaled from RPM 1 to RPM 2 comparing to a PWL spectrum directly measured at RPM 2. In general, for all cv analyzed and at both angles of attack, the calculated spectra of PWL have a good agreement with experimental results, which shows that the acoustic similarity methodology adopted in this work is able to calculate the $\beta(\varphi)$ and $F(St,\varphi)$ even for the present large-scale fan model. However, the PWL calculated at ANG 2 - cv3 and ANG 2 - cv4 are slightly underpredicted at frequencies higher than 2 kHz. Probably this is happening because of the difference of the airflow coefficient value inside the cv3 and cv4 ranges which have larger values for experiments performed at ANG 2 at RPM 1. As mentioned before, the difference between airflow coefficient values can change the high frequency noise, leading to a small errors in PWL scaling in this case.

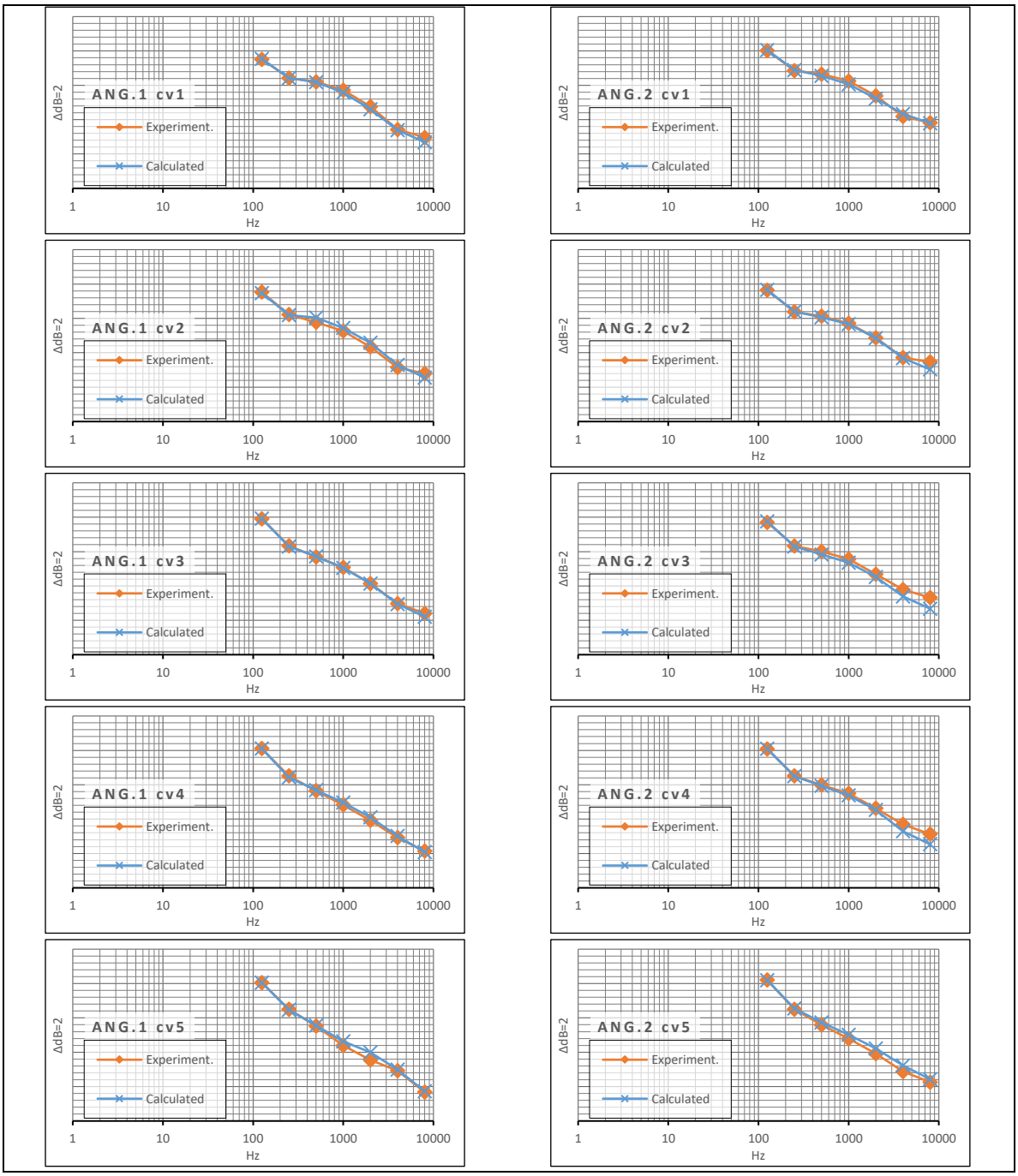

Figure 5: Comparison between PWL calculated for RPM 2 and PWL measured in the experiments.

In Eq. (11), $F(St,\varphi)$ represents the spectral distribution of sound generated by the aeroacoustic phenomena and it can be split in two parts: the discrete noise components and random noise. The discrete noise is usually related to tonal frequencies, i.e, for integer numbers of St, because of the fan blade passing frequency, while the random noise is related to fractions of St number since its source is turbulence. However, in this work the results presented in Figs. 6 and 7 have the contribution of both components. The spectra of $10\log_{10} F(St,\varphi)$ in Fig. 6 has, in practice, the same slope for both blade angles and cv values but do not have the same gap between the blade angles. The curves of ANG 1, for all cv, have larger values than those observed for ANG 2, which means that, when the blade angle increases, the value of $10\log_{10} F(St,\varphi)$ becomes more relevant in Eq. (13), changing with cv value. Now, keeping the same blade angle and changing the values of cv, Fig. 7 shows that the value of $10\log_{10} F(St,\varphi)$ decreases when cv decreases. This happens only for ANG 1 from cv1 to cv4 and, for ANG 2, a more complicated behavior is observed. Neise and Barsikow (1982) found the same behavior for the values of $10\log_{10} F(St,\varphi)$ presented in this work for ANG 1 but their study was related to centrifugal fans where the blade angle was kept constant.

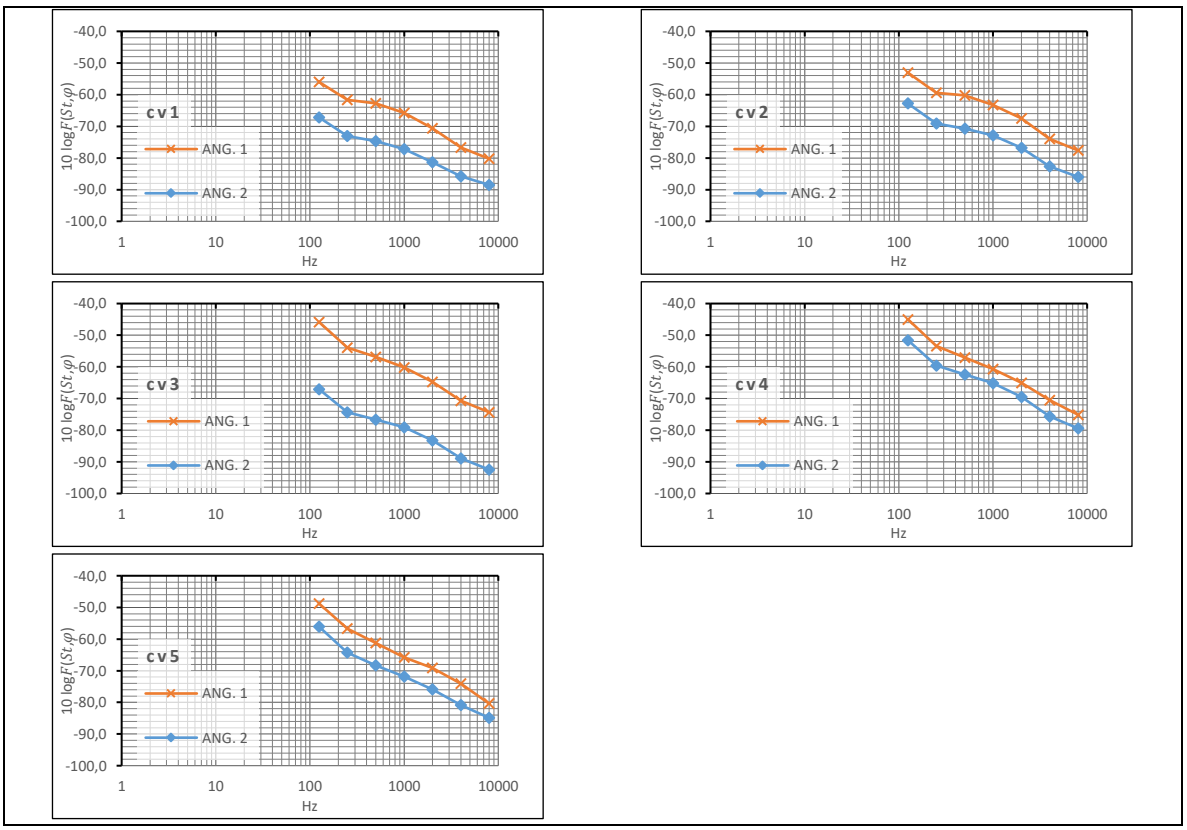

Figure 6: Comparison of $10\log_{10} F(St,\varphi)$ values calculated for ANG 1 and ANG 2 at each cv range.

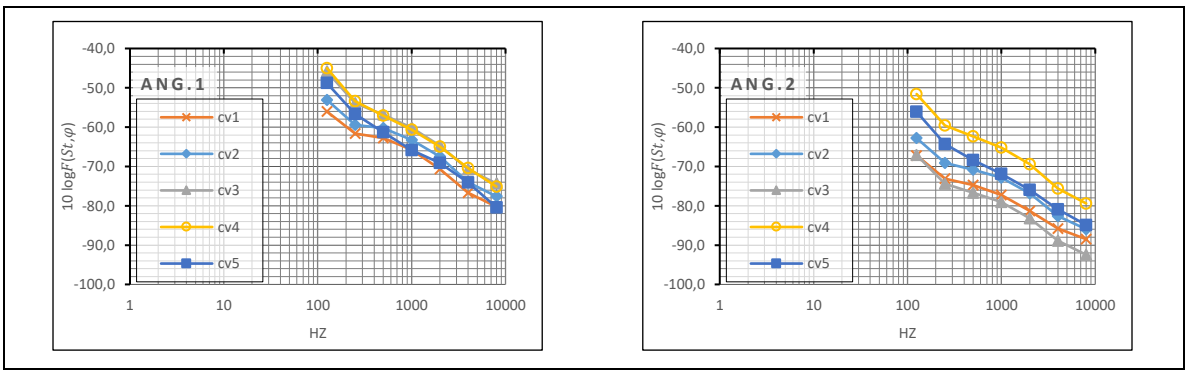

Figure 7: Comparison of $10\log_{10} F(St,\varphi)$ values calculated for the entire cv range and each angle of attack.

4. CONCLUSIONS

An acoustic similarity study is performed for an industrial fan of 10,97 m diameter using experimental measurements of sound pressure level. Experiments are conducted for a fan operating at five different air flow conditions, two-blade angle configurations and two rotational speeds. The acoustic data are treated as sound power level and its calculation from sound pressure level is performed following the ISO 3747 procedures as it is briefly detailed and discussed. In the scaling study, the procedure used to obtain relevant parameters such as the Mach number coefficient $\beta(\varphi)$ and the spectral function $F(St,\varphi)$ is shown and discussed.

The PWL spectra is measured with the fan operating at one rotation and the scaling is performed using the $\beta(\varphi)$ and $F(St,\varphi)$ functions. Then, a new PWL spectra is calculated considering a different rotation. This procedure is performed for all air flow and pitch angles of the blade. The results show that the calculated spectra of PWL have a good agreement with experimental spectra of PWL measured at the second rotation for all air flow points and pitch angles of the blade. Thus, it is possible to conclude that the procedure developed here provides a good model for the present large-scale fan type. Moreover, the calculated values of the $\beta(\varphi)$ and $F(St,\varphi)$ functions seem to be reliable to analyze

the fan behavior when the air flow and pitch angle of the blade are changed, which is one of the main goals of this work.

The results obtained in this work show that $\beta(\varphi)$ and $F(St,\varphi)$ are considerably influenced by the air flow coefficient and pitch angle of blade. The Mach coefficient $\beta(\varphi)$ has a linear behavior as function of the air flow coefficient when the angle is kept constant. When the results of two pitch angles are analyzed, the distribution of the $\beta(\varphi)$ has almost the same slope but with a shift depending on the angle. The higher angle of attack displaying lower values of $\beta(\varphi)$. The values found here range from 1,5 up to 4,3 considering both angles tested. These values are close to the value of 2 suggested in literature for general fan scaling purposes. From the present study, it is found that a universal value of $\beta(\varphi)$ should not be used since it can compromise the accuracy of the overall PWL up to 1.8 dB. The values of $F(St,\varphi)$ for the lowest pitch angle also display a shift in magnitude while keeping the same slope when the air flow coefficient is kept constant. However, these shifts do not follow a pattern when the air flow coefficient is changed. For the lower angle of attack tested, there is a trend that $F(St,\varphi)$ values increase when the air flow coefficient increases, but the behavior is more complex when the angle of attack is increased.

It is possible to conclude that $\beta(\varphi)$ and $F(St,\varphi)$ should be obtained through an experimental approach to achieve accurate PWL calculations. As they are a strong function of air flow and pitch angle of the blade, a further analysis should be done to determine the $\beta(\varphi)$ and $F(St,\varphi)$ for other pitch angles in order to observe if the behavior observed here for these functions is kept the same.

5. REFERENCES

AMCA 210-16, 2016, Laboratory Methods of Testing Fans for Certified Aerodynamic Performance Rating.

Barron, R. F., 2001, *Industrial Noise Control and Acoustics.* New York : Marcel DEkker, Inc.

Blake, W. K., 2017, *Mechanics of flow-induced sound and vibration*, Academic Press, 4th edition.

Bleier, F. P., 1997, *Fan Handbook. Selection: application and design*, Mc Graw Hill.

Cattanei, A., Canepa, E., 2011, Analysis of the SPL Spectra Generated by Axial Flow Fans Working Under Similarity Conditions, *32nd AIAA Aeroacoustics Conference*, *AIAA Paper* 2011-2872.

ISO3747., 2010, Determination of sound power levels of noise sources using sound pressure - Comparison method in situ.

Kinsler, L. E., 2000, *Fundamentals of Acoustics.* New York : Jhon Wiley & Sons, 4th edition.

Neise, W. and Barsikow, B., 1982. Acoustic Similarity Laws for Fans, *ASME Journal of Engineering for Industry*, 104: 162-168.